

Review

Manufacturing High-Energy-Density Sulfidic Solid-State Batteries

Gang Li ¹, Shuo Wang ^{2,3,*}, Jipeng Fu ⁴, Yuan Liu ^{5,*} and Zehua Chen ^{6,*}¹ School of Naval Architecture, Ocean and Energy Power Engineering, Wuhan University of Technology, Wuhan 430070, China; hbxylg88@163.com² Center of Smart Materials and Devices, State Key Laboratory of Advanced Technology for Materials Synthesis and Processing & School of Material Science and Engineering, Wuhan University of Technology, Wuhan 430070, China³ Foshan (Southern China) Institute for New Materials, Foshan 528200, China⁴ Key Laboratory of Rare Earth Optoelectronic Materials and Devices of Zhejiang Province, Institute of Optoelectronic Materials and Devices, China Jiliang University, Hangzhou 310018, China; fujipeng@cjlu.edu.cn⁵ College of Materials Science and Engineering, Qingdao University, Qingdao 266071, China⁶ Institute of New Energy Battery, Yibin Vocational & Technical College, Yibin 644003, China

* Correspondence: shuowang@whut.edu.cn (S.W.); liuyuan@qdu.edu.cn (Y.L.); chenzh2016@126.com (Z.C.)

Abstract: All-solid-state batteries (ASSBs) using sulfide solid electrolytes with high room-temperature ionic conductivity are expected as promising next-generation batteries, which might solve the safety issues and enable the utilization of lithium metal as the anode to further increase the energy density of cells. Most researchers in the academic community currently focus on developing novel sulfide solid electrolytes, clarifying the interface issues between sulfide electrolytes and solid electrodes and mechanism of lithium dendrite growth in ASSB. However, there is a lacking in the technical route analysis about the commercialization of ASSBs based on sulfide solid electrolytes. This review mainly introduces the specific preparation methods of various parts in sulfide-based ASSBs, including the preparation methods of sulfide solid electrolyte particles, sulfide-based composite electrolyte membranes, composite cathodes and anodes, and analyzes the advantages and disadvantages of these methods. In addition, several schemes of ASSB assembly are also introduced. Finally, a perspective of large-scale production of sulfide-based ASSBs is provided, which is expected to accelerate the commercialization of sulfide-based ASSBs.



Citation: Li, G.; Wang, S.; Fu, J.; Liu, Y.; Chen, Z. Manufacturing High-Energy-Density Sulfidic Solid-State Batteries. *Batteries* **2023**, *9*, 347. <https://doi.org/10.3390/batteries9070347>

Academic Editor: Claudio Gerbaldi

Received: 23 May 2023

Revised: 21 June 2023

Accepted: 25 June 2023

Published: 28 June 2023



Copyright: © 2023 by the authors. Licensee MDPI, Basel, Switzerland. This article is an open access article distributed under the terms and conditions of the Creative Commons Attribution (CC BY) license (<https://creativecommons.org/licenses/by/4.0/>).

1. Introduction

Lithium-ion batteries are widely used in portable electronic devices, such as mobile phones, cameras, laptops and other electronic products, due to their high energy density and light weight [1]. To reduce carbon emissions, the new energy electric vehicle industry has shown a spurt of development in recent years [2]. The commercial lithium-ion batteries with flammable organic liquid electrolytes are easy to burn and explode in case of damage, and lithium dendrites are easy to grow when the cells are cycled at a high current density, which will pierce the separator, cause a short circuit and pose a serious safety hazard [3–5]. In addition, when matched with a high-nickel ternary cathode, the oxidation of the liquid electrolyte and the dissolution of transition metal ions will also shorten the battery life [6,7]. In liquid lithium–sulfur batteries, the polysulfide shuttle effect results in low coulombic efficiency and rapid capacity decay [8]. Developing next-generation lithium-ion batteries with high energy density, high power density and high safety has become a research hotspot in the field of lithium-ion batteries in the future.

Replacing commercial liquid electrolytes and separators with solid electrolytes could improve the safety property of the batteries and enable the utilization of lithium metal as the anode to further increase the energy density of cells [9,10]. Solid electrolyte is the core component of SSBs, which gains great attention. The solid electrolytes could be classified as polymer-based electrolytes, inorganic electrolytes, and organic–inorganic composite electrolytes [11–13]. Generally, solid polymer-based electrolytes show good flexibility and processability, but the room-temperature ionic conductivity is low (10^{-6} – 10^{-4} S cm $^{-1}$). The inorganic solid electrolytes could be divided into oxides, halides, and sulfides according to their composition. Compared with other inorganic solid electrolytes, the ionic conductivity of sulfide electrolytes has reached a high level, and it even exceeds their liquid electrolyte counterparts [14–19]. Moreover, the sulfide electrolyte is soft and easy to be cold-pressed, which gains discernible attention [20]. The thermal stability of the sulfide electrolytes is also good; therefore, the working temperature of the sulfide-based all-solid-state battery (ASSB) ranges from –30 °C to 100 °C [15]. When combining with the high-voltage cathode material, the voltage of the cell is expected to increase to 5 V for further increasing the energy density of the whole cell [21]. When sulfide electrolytes combine with high-capacity cathode material such as sulfur, the shuttle effect of polysulfides could be suppressed, thereby improving the Coulombic efficiency of the cell [22]. Theoretical calculations reveal that, only when the ionic conductivity of the solid electrolyte in the composite cathode reaches 10^{-2} S cm $^{-1}$, the performance of ASSBs could be comparable to that of the commercial lithium-ion battery [23]. Some experimental results also show that the ionic conductivity of solid electrolyte affects the effective ionic conductivity of the composite cathode, thereby affecting the cycling and rate performance of ASSBs [24,25]. Compared with sulfide electrolytes, the ionic conductivity of polymers and oxides is too low to meet the requirements. Kanno et al. reported that a sulfide ASSB could be cycled at a large current density at –30 and 100 °C [15], which is difficult to be achieved in polymer-based or oxide-based ASSBs. Thus, sulfide electrolytes are expected to be successfully applied to ASSBs in the future.

Different from the commercial lithium-ion battery in which the organic electrolyte could penetrate the composite cathode, solid electrolyte is required to be added into the composite cathode for the ASSBs to provide lithium transport pathways [24,26]. Therefore, the design and manufacture of the composite cathode will be more complicated. Commercial lithium-ion batteries are often produced via roll-to-roll and liquid electrolyte injection, while the assembly of ASSBs requires technological innovation on this basis. There are many review articles focusing on the introduction of classification, ionic conductivity and air stability of sulfide solid electrolyte, chemo-mechanical effects, interface issues, and lithium dendrite growth in sulfide-based SSBs [11,20,27–29]. Herein, we will not introduce them in detail.

In this review, we mainly focus on the introduction of preparation and production methods, challenges, and prospects of SSBs based on sulfide solid electrolytes. The preparation methods of sulfide electrolyte particles, sulfide–polymer composite electrolyte membranes, composite cathodes and anodes, and the assembly method of full cells are introduced in detail (Figure 1). In addition, the advantages and disadvantages of these methods are analyzed, and the future development direction of ASSBs are pointed out, which will help to accelerate the commercialization of sulfide-based ASSBs.

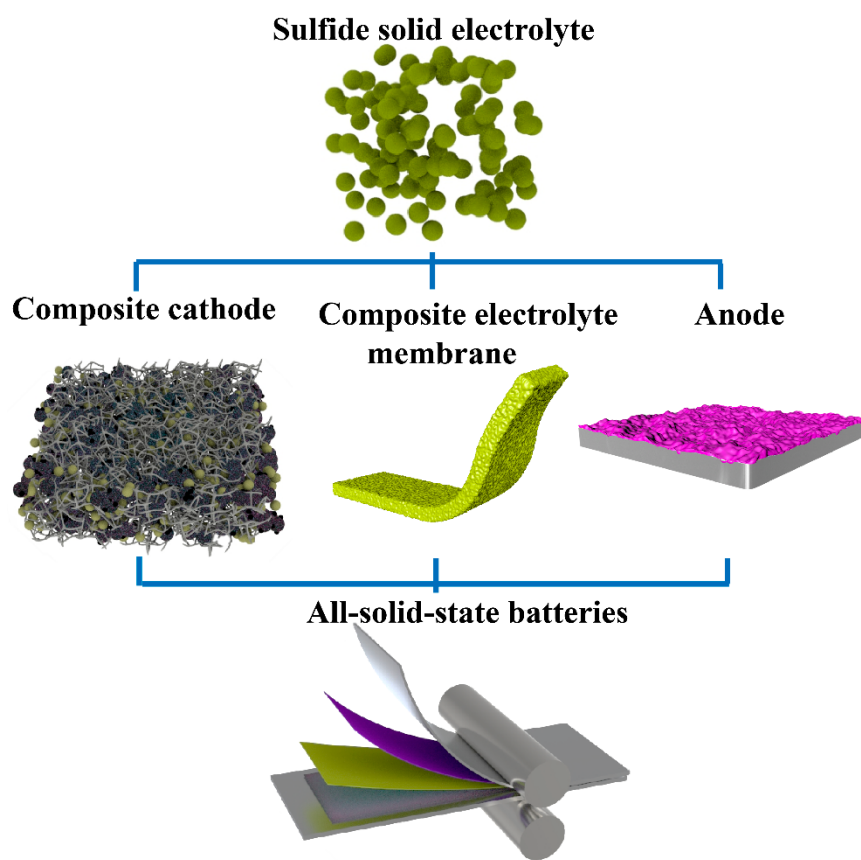


Figure 1. Schematic illustration of the key components of ASSBs. Firstly, the sulfide solid electrolyte is prepared, and then the composite electrode and composite electrolyte membrane are prepared, and finally an ASSB is assembled.

2. Sulfide Solid Electrolyte Processing

Since sulfide solid electrolytes are sensitive to water and oxygen in the air, they are usually prepared under an inert atmosphere. The preparation methods of sulfide solid electrolytes include melt-quenching, high-energy ball milling, liquid-phase reaction, and solid-state reaction. We will briefly introduce these methods below.

(1) Melt-quenching

The specific process of melt-quenching is as follows [30–33]. Firstly, the raw materials (such as Li_2S (99.9%, ~200 mesh powder) and P_2S_5 (99%, powder)) are mixed, pressed into pellets and sealed in the carbon-coated quartz tubes, and then heat-treated at high temperature to a molten state. Finally, the melt is quickly quenched in liquid nitrogen to obtain glassy sulfide solid electrolytes. The room-temperature ionic conductivity prepared via melt-quenching is usually about 0.1 mS cm^{-1} . The highest ionic conductivity could reach 1 mS cm^{-1} ; however, melt-quenching is complex, time-consuming and energy-consuming [34].

(2) Liquid-phase synthesis

The liquid-phase synthesis has some advantages of low cost, time-saving, and uniformity, but the obtained room-temperature ionic conductivity of the sulfide solid electrolytes is relatively low. Liquid-phase methods include suspension synthesis and dissolution-precipitation [35] (Figure 2a). The suspension synthesis method is that the precursors are added to a solvent and stirred until the reaction finishes, and then the solvent is evaporated to dryness and heat-treated to obtain sulfide solid electrolyte powder.

For example, Li_2S and P_2S_5 were added to tetrahydrofuran, stirred and reacted to form a suspension, then Li_2S and LiCl were dissolved in absolute ethanol and stirred. Next, the two solutions were stirred, evaporated to dryness, and heat-treated at 550°C . Finally, the

$\text{Li}_6\text{PS}_5\text{Cl}$ electrolyte containing a small amount of Li_3PO_4 impurity was obtained. However, the utilization of a mixed solution of acetonitrile and 1-propanethiol to prepare $\text{Li}_6\text{PS}_5\text{Cl}$ could avoid the nucleophilic reaction and eliminate the Li_3PO_4 impurity, thereby further improving the ionic conductivity of the $\text{Li}_6\text{PS}_5\text{Cl}$ electrolyte and reducing the activation energy [36]. In addition, some new electrolytes could also be obtained via liquid-phase synthesis, such as $\text{Li}_7\text{P}_2\text{S}_8\text{I}$, which shows an ionic conductivity of $6.3 \times 10^{-4} \text{ S cm}^{-1}$ and good stability against lithium anode [37].

The process of the dissolution–precipitation method is as follows. First, the sulfide solid electrolyte prepared by solid-state reaction or high-energy ball milling is dissolved into a polar solvent, stirred and evaporated to dryness, and finally annealed at a certain temperature to obtain the final solid electrolyte powder [35]. Using the dissolution–precipitation method could obtain some new solid electrolytes which are difficult to be synthesized by traditional solid-state reaction. For example, LiI and Li_4SnS_4 were dissolved in methanol solution, stirred and evaporated to dryness, and finally heat-treated at 200°C to obtain $0.6\text{LiI}\cdot0.4\text{Li}_4\text{SnS}_4$ electrolyte. This amorphous electrolyte is stable in dry air and is softer than crystalline Li_4SnS_4 [38].

(3) High-energy ball milling

High-energy ball milling is usually carried out at room temperature, and some new glassy sulfide electrolytes could be prepared via this method. However, high-energy ball milling is time-consuming [39–41]. Especially, the milling speed and durations have an important role in the phase composition and crystallinity of the solid electrolytes. Taking $\text{Li}_6\text{PS}_5\text{Cl}$ electrolyte as an example, when the milling speed is lower than 110 rpm, the amorphous compound will not form. When the milling speed reaches 550 rpm and the ball-milling duration reaches 4 h, the high conductive $\text{Li}_6\text{PS}_5\text{Cl}$ phase begins to form, and as the ball-milling time exceeds 8 h, the ionic conductivity will no longer increases. Subsequent annealing after high-energy ball milling could further improve the crystallinity of the solid electrolyte and further increase the ionic conductivity of solid electrolyte [42]. For example, Yu et al. mixed Li_2S , P_2S_5 and LiBr according to an appropriate ratio, and the $\text{Li}_{5.5}\text{PS}_{4.5}\text{Br}_{1.5}$ electrolyte with a high ionic conductivity of 4.2 mS cm^{-1} was obtained through high-energy ball milling followed by annealing [43].

(4) Solid-state reaction method

Solid-state reaction is a popular method to obtain crystalline sulfide solid electrolytes. Specifically, the raw materials are dry-mixed, pressed into pellets, sealed in high vacuum, and then heat-treated, and finally the ceramic pellets are ground to fine solid electrolyte powder. In recent years, the room-temperature ionic conductivity of crystalline sulfide electrolytes prepared via solid-state reaction is very high, and some even exceed the level of liquid electrolytes, such as $\text{Li}_{6.6}\text{P}_{0.4}\text{Ge}_{0.6}\text{S}_5\text{I}$ (5.4 mS cm^{-1}) [44], LGPS (12 mS cm^{-1}) [14], $\text{Li}_{6.6}\text{Si}_{0.6}\text{Sb}_{0.4}\text{S}_5\text{I}$ ($1.48 \times 10^{-2} \text{ S cm}^{-1}$) [16], etc. Recent researchers have revealed that compared with high-energy ball milling followed by annealing, comparable ionic conductivity of the chlorine-rich lithium argyrodites could also be obtained via rapid dry-mixing followed by annealing. Prolonging annealing duration will lead to the volatilization of lithium, resulting in a decrease of ionic conductivity. The $\text{Li}_{5.5}\text{PS}_{4.5}\text{Cl}_{1.5}$ electrolyte with an ionic conductivity of 8.3 mS cm^{-1} could be achieved by annealing at 450°C for 3 h. This will greatly improve the production efficiency and provide a theoretical and experimental fundament for large-scale manufacturing [45] (Figure 2b).

The particle size distribution (PSD) of sulfide solid electrolytes has an important impact on the electrochemical performance of ASSBs. The use of smaller PSD of sulfide solid electrolyte in composite cathode will increase ionic percolation and reduce tortuosity, thereby improving the utilization of active materials, cycling life and rate performance of ASSBs [46]. Using high-energy ball milling will reduce the PSD of the sulfide electrolyte; however, it will make the surface of the sulfide electrolyte amorphous and reduce the ionic conductivity of the sulfide electrolyte [47]. In addition, the PSD of the obtained sulfide electrolyte is not uniform, generally from several hundred nanometers to several microns [48]. Wet ball-milling could be used to reduce the PSD of sulfide electrolytes to

the submicron level, and a more uniform PSD could be achieved. Since the thiophosphate electrolyte will decompose in polar solvents, weaker or nonpolar solvents, such as toluene, p-xylene, and heptane, are preferentially selected. After wet grinding, the solvent is evaporated to dryness, and then the electric screen is used to filter out the larger sulfide electrolyte to obtain the smaller particles [49] (Figure 2c). However, the ionic conductivity will be sharply reduced after wet milling. Therefore, it is necessary to develop more advanced technologies to prepare smaller sulfide electrolyte particles with higher ionic conductivity.

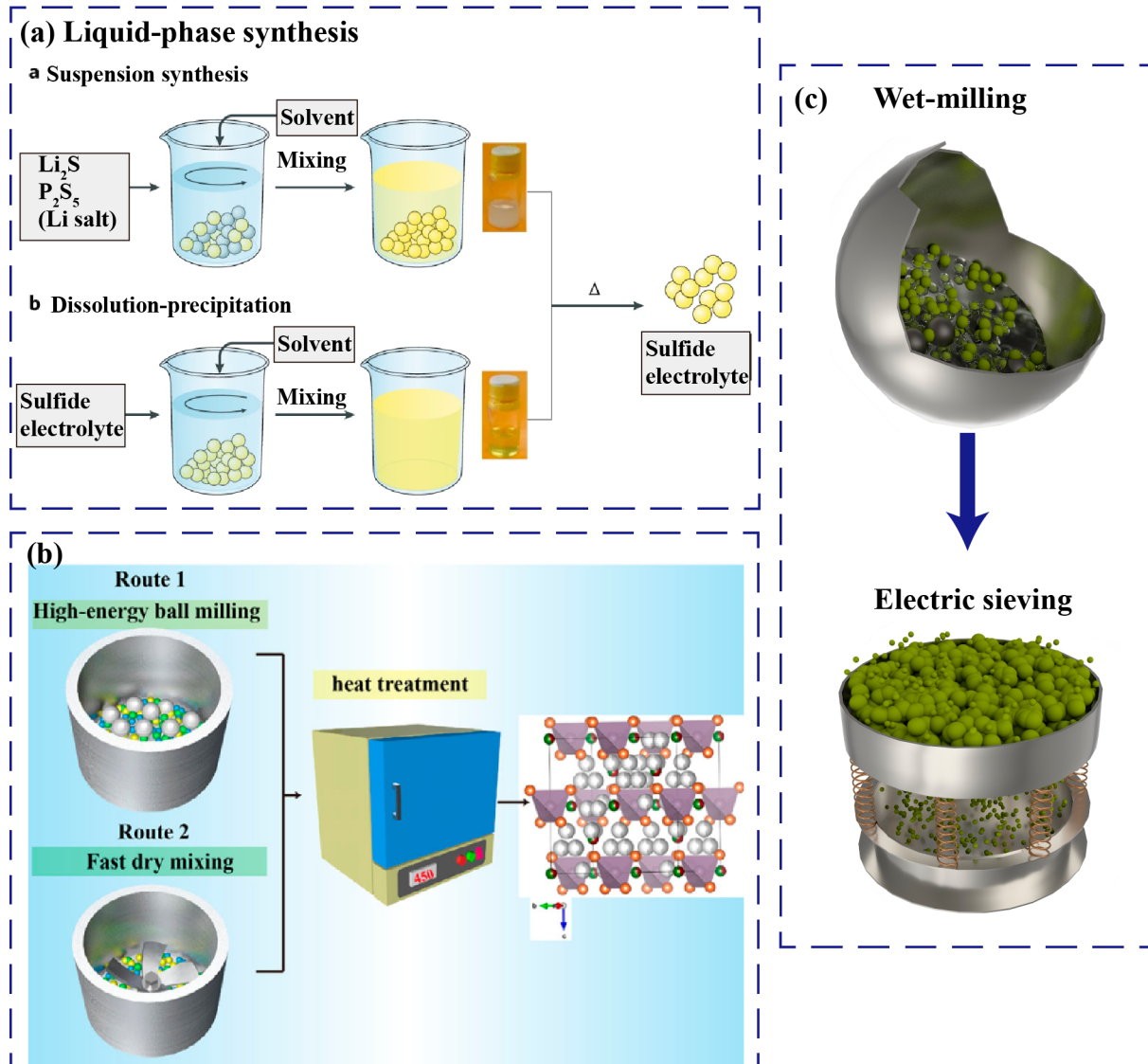


Figure 2. (a) Schematic diagram of two liquid-phase syntheses routes for sulfide electrolytes, including suspension synthesis and dissolution–precipitation. Reproduced with permission from Ref. [35]. Copyright 2019, Springer Nature; (b) Schematic diagram of two synthesis routes for halogen-rich lithium argyrodite, including high-energy ball milling followed by annealing, and fast dry-mixing followed by heat treatment. Reproduced with permission from [45]. Copyright 2023, John Wiley and Sons; (c) Schematic diagram of reducing PSD of sulfide solid electrolyte by wet milling followed by electric sieving.

The room-temperature ionic conductivity of the sulfide solid electrolytes prepared by melt-quenching or high-energy ball milling is relatively low. However, solid-state reaction or liquid-phase synthesis are suitable for large-scale preparation of sulfide solid electrolytes

with high ionic conductivity (see Table 1). Since the liquid-phase method requires the utilization of toxic solvents and more time to evaporate the solvents, solid-state reaction is therefore more suitable for manufacturing sulfide solid electrolyte powders.

Table 1. Comparison of ionic conductivity, time consumption and production capacity of different preparation methods of sulfide electrolyte powder.

Preparation Method	Ionic Conductivity	Time Consumption	Product Capacity
Melt-quenching	★★	★★★	★
Liquid-phase synthesis	★★★★	★★★★	★★★★★
High-energy ball milling	★★★	★★★★★	★★★
Solid-state reaction	★★★★★	★★★	★★★★★

3. Manufacturing of Composite Solid Electrolyte

Due to the brittle property of sulfide electrolyte ceramics, the thickness of the solid electrolyte layer is in the range of 0.6–1 mm during cell assembly. Reducing the thickness of the solid electrolyte layer will help to increase the specific energy of the whole cell. Adding polymer binder in the sulfide electrolyte matrix is expected to obtain a composite electrolyte membrane with high ionic conductivity and good flexibility at the same time [26]. Recently, the preparation methods of sulfide–polymer composite electrolyte membrane mainly include dry process and wet process.

Regarding the dry preparation, one is that the sulfide electrolyte is mixed with a small amount of polymer binder via ball milling to obtain a composite electrolyte powder, and then the powder is cold-pressed to form a ceramic sheet. The thickness of the obtained sheet is usually around 60–100 μm [50,51]. Although the composite electrolyte membrane is freestanding, it is not flexible, and the polymer binder will easily agglomerate during the dry process, which hinders the ionic transport pathways and reduces the ionic conductivity. Therefore, the ionic conductivity of the obtained composite electrolyte membrane is typically around 0.1 mS cm^{-1} . For example, the $77.5\text{Li}_2\text{S}\text{-}22.5\text{P}_2\text{S}_5$ glass ceramics and polyimide were mixed via ball milling, and then the milled composite powder was hot-pressed to obtain a freestanding sheet with a thickness of $63.7 \mu\text{m}$ and an ionic conductivity of about $1 \times 10^{-4} \text{ S cm}^{-1}$ [51].

Recently, another new dry process method has emerged. The sulfide electrolyte is mixed with the polymer binder, and the polymer fibrillates under shear force to form a porous polymer network that acts as a bond to the solid electrolyte particles. Zhang et al. mixed $\text{Li}_{5.4}\text{PS}_{4.4}\text{Cl}_{1.6}$ with a small amount of polytetrafluoroethylene (PTFE) by low-speed ball milling, and then a $\text{Li}_{5.4}\text{PS}_{4.4}\text{Cl}_{1.6}\text{-PTFE}$ composite electrolyte membrane with a thickness of $30 \mu\text{m}$ and an ionic conductivity of about 8.4 mS cm^{-1} at room temperature was prepared by hot rolling [52] (Figure 3a). Similarly, Wang et al. prepared a $\text{Li}_6\text{PS}_5\text{Cl}\text{-PTFE}$ composite electrolyte membrane with a thickness of $20 \mu\text{m}$ and a room-temperature ionic conductivity higher than 1 mS cm^{-1} [53]. The composite electrolyte membranes using PTFE as binder show high ionic conductivity at room temperature; however, the PTFE is unstable against lithium metal anode and easy to decompose, resulting in capacity degradation of ASSBs. Therefore, it is necessary to modify the interface between lithium anode and composite electrolyte to suppress interfacial side reactions.

Regarding the wet process, one is that the polymer binder was half-dissolved into an organic solvent, then the sulfide electrolyte was added and evaporated to obtain composite electrolyte powders, and then cold-pressed to form a composite electrolyte membrane. Compared with ball milling, using this wet process will obtain more uniform dispersion of polymer binders and higher ionic conductivity of about $0.5\text{--}1 \text{ mS cm}^{-1}$, but the thickness is still $100\text{--}120 \mu\text{m}$ [54]. Another is that nonwoven or polymer binder network prepared via electrospinning is used as a support, and sulfide electrolyte slurry was infiltrated into the pores, or doctor-bladed on the support, and then cold-pressed to obtain a composite electrolyte membrane. This method can avoid the sulfide electrolyte being completely

covered by the polymer, and it is expected to obtain a higher room-temperature ionic conductivity membrane [55–57]. Kim et al. recently prepared porous polyimide (PI) by electrospinning technology and infiltrated with $\text{Li}_6\text{PS}_5\text{Cl}_{0.5}\text{Br}_{0.5}$ -ethanol solution (Figure 3b). Then, the slurry was evaporated and heat-treated at $400\text{ }^\circ\text{C}$ to obtain a flexible freestanding composite electrolyte membrane with a thickness of $40\text{ }\mu\text{m}$ and room-temperature ionic conductivity of 0.058 mS cm^{-1} [58]. Similarly, a poly (vinylidene fluoride-co-trifluoroethylene) network was prepared by electrospinning, and infiltrated with $\text{Li}_6\text{PS}_5\text{Cl}$ suspension in toluene, and then the membrane was hot-pressed to obtain a flexible freestanding composite electrolyte with a thickness of $30\text{ }\mu\text{m}$ and an ionic conductivity of 1.2 mS cm^{-1} at room temperature [59].

Recently, one of the most popular wet process methods is tape casting [60,61], that is, the binder is dissolved in a nonpolar solvent or a weak-polar solvent, and then the sulfide electrolyte is added to the solvent and stirred until the sulfide electrolytes disperse uniformly in it. Finally, the slurry is tape-casted and evaporated to obtain a composite electrolyte membrane (Figure 3c). Adopting the tape-casting method could obtain the composite electrolyte membranes on a large scale [62]. However, the sulfide electrolyte particles will be easily wrapped by polymers, thereby increasing the tortuosity of lithium-ion diffusion and reducing the ionic conductivity of the sulfide solid electrolyte [63,64]. Using more binders will help to prepare thinner electrolyte membranes. However, they will seriously hinder the ionic conduction, resulting in poor rate performance. Using a more cohesive polymer binder could reduce the usage amount of binder, which helps to obtain a thinner composite electrolyte membrane with higher room-temperature ionic conductivity [65].

In short, the tape-casting is currently the most suitable method for large-scale preparation of composite electrolyte membranes. However, considering the use of toxic solvents and the environmental pollution caused by solvent volatilization, as well as the low ionic conductivity of sulfides, once the dry process equipment and novel binders make new breakthroughs, the dry process is more likely to be widely used in large-scale preparation of thin composite electrolyte membrane with high room-temperature ionic conductivity in the future.

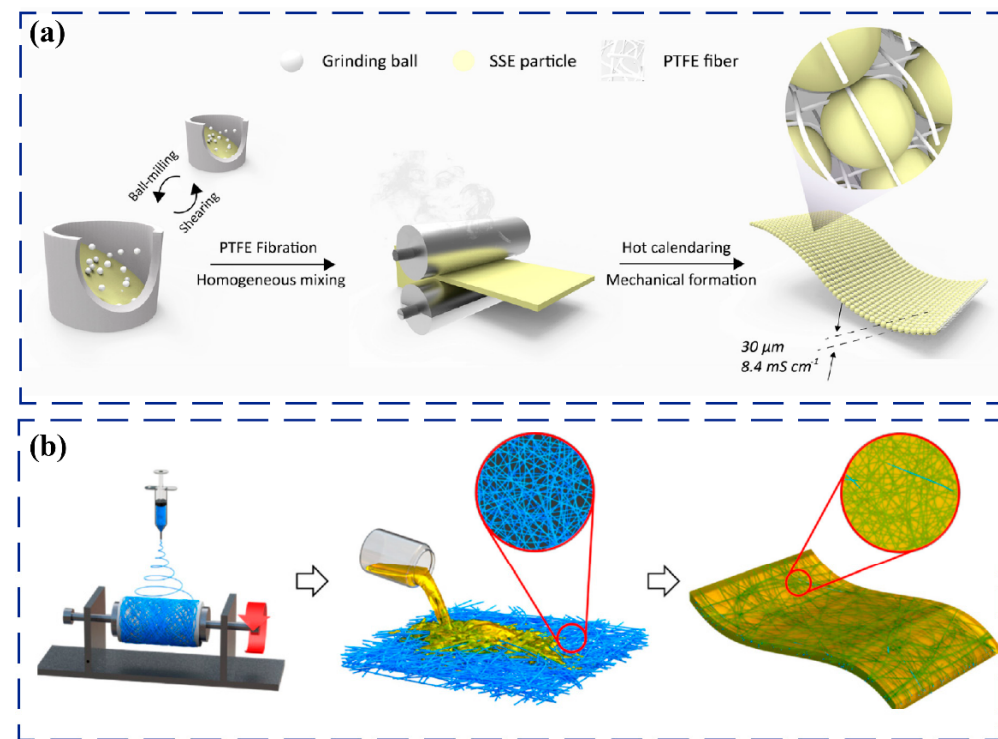


Figure 3. Cont.

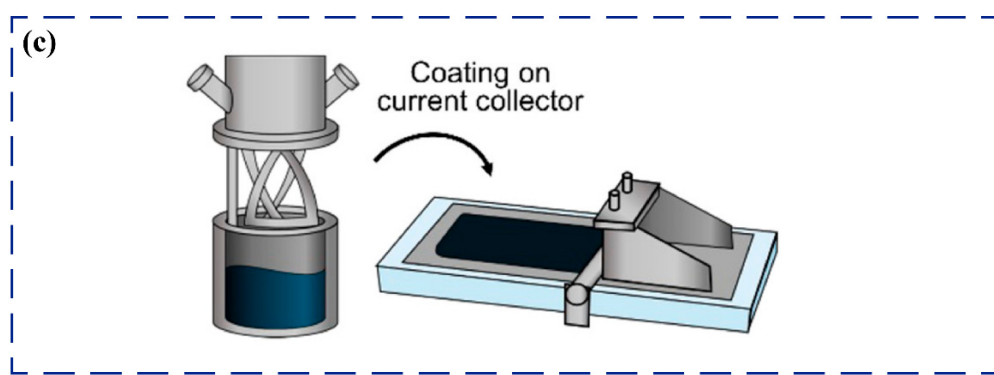


Figure 3. (a) Schematic illustration of the dry process of ultrathin sulfide/PTFE composite membrane. Reproduced with permission from [52]. Copyright 2021, American Chemical Society; (b) Schematic illustrating the preparation of composite electrolyte membranes for ASSBs by infiltration of electro-spun porous PI network with solution-processable $\text{Li}_6\text{PS}_5\text{Cl}_{0.5}\text{Br}_{0.5}$. Reproduced with permission from [58]. Copyright 2020, American Chemical Society; (c) Schematic illustration of the preparation of sulfide-based composite electrolyte membrane by tape-casting method. Reproduced with permission from [62]. Copyright 2021, American Chemical Society.

4. Composite Cathode Fabrication

Different from liquid lithium-ion batteries, a large amount of solid electrolyte needs to be added to the composite cathodes for ASSBs to play a role of ionic transport [66–68]. Recently, dry process is widely used to prepare composite cathodes in most laboratories. Specifically, active materials, electronic conductive agents, and sulfide electrolytes are mixed by hand or ball-milled to obtain composite cathodes powders [69].

When the oxide electrode material is used as cathode-active material, to suppress the space charge layer and side reactions at the high-nickel ternary cathode/sulfide electrolyte interface, the cathode material is usually coated [27]. To avoid damage of the coating caused by ball milling, manual grinding is generally used [70]. However, when elemental sulfur or metal sulfide is used as the active material, the composite cathode prepared by ball milling exhibits better electrochemical performance compared with manual grinding. It is found that due to the large volume change of sulfur during charge and discharge, chemo-mechanical failure occurs in the composite cathode obtained by manual grinding, resulting in poor contact and irreversible Li_2S formation. However, smaller sulfur active material could be obtained through ball milling, which will minimize the drastic volume change of cathode-active material, thereby increasing the specific capacity and capacity retention of the cells [71]. The obtained composite cathode powder is usually spread on one side of the solid electrolyte layer and cold-pressed during the assembly process of ASSBs [72]. This dry method could be used to investigate the effect of coatings on cathode-active materials and the electro-chemo-mechanical effects of the composite cathode; however, it is difficult to manufacture composite cathodes on a large scale.

With Tesla's announcement of the dry electrode process, dry process of composite cathodes for sulfide-based ASSBs has also attracted attention. The detailed process is as follows. First, the oxide cathode-active materials, conductive carbon, and sulfide electrolyte are dry-mixed, and then PTFE is added for further dry mixing. Finally, the mixture is hot-rolled to obtain a composite cathode (Figure 4a). The dry process shows great promise due to its simple process, solvent-free preparation and ability to fabricate thicker electrodes. For example, Stefan et al. reported an ASSB which achieved a high areal capacity of 6.5 mAh cm^{-2} with a small amount of polymer binder [73].

The wet method is also a promising method for large-scale preparation of composite cathode sheets. One is the sulfide electrolyte solution-infiltrated electrode method, that is, the ethanol solution of sulfide electrolyte is infiltrated into commercial electrode and then solidified. For example, commercial composite electrode is prepared by the tape-

casting method, that is, LiNbO_3 -coated LiCoO_2 , super P and polyvinylidene fluoride (PVDF) binder are added to N-methylpyrrolidone solution, and then stirred, coated on the current collector, and finally the solvent is evaporated to dryness to obtain a commercial electrode. Since the PVDF binder in the composite cathode is unstable at high temperature, the $\text{Li}_6\text{PS}_5\text{Cl}$ -infiltrated electrode is heat-treated at $180\text{ }^\circ\text{C}$. The ionic conductivity of the obtained $\text{Li}_6\text{PS}_5\text{Cl}$ ($1.9 \times 10^{-4}\text{ S cm}^{-1}$) is lower than that of the $\text{Li}_6\text{PS}_5\text{Cl}$ annealing at $550\text{ }^\circ\text{C}$ ($3 \times 10^{-3}\text{ S cm}^{-1}$), which leads to low effective ionic conductivity and poor rate performance [74]. Therefore, the sulfide electrolyte system whose ionic conductivity could be recovered after being dissolved in a polar solvent and evaporated to dryness is more suitable for this method.

Tape casting is a method that could be used to prepare composite cathodes for SSBs on a large scale (Figure 4b). Specifically, the active material, conductive carbon (such as super P), sulfide electrolyte, and binder with less electronegativity (such as poly(acrylonitrile-co-butadiene), polystyrene-block-poly-butadiene or styrene-ethylene-butylene-styrene) are added to a nonpolar or weakly polar solvent, stirred to form a slurry, and then coated on the current collector and evaporated to dryness [75]. Generally, the ionic conductivity of the sulfide electrolytes will decrease when they are mixed with insulating polymer binder, which distributes along the grain boundaries and hinders the ionic conduction [76]. Therefore, optimizing the ratio between different components of the composite cathode and improving the mixing process are very important for ASSBs to achieve excellent performance.

In short, like the preparation of composite electrolyte membranes, tape casting is currently the most applicable method for large-scale preparation of composite cathodes. However, once new breakthroughs have been made in dry-process preparation equipment and new binders, the dry process is expected to be widely used in large-scale preparation of composite cathodes in the future, which will greatly improve production efficiency and be environmentally friendly.

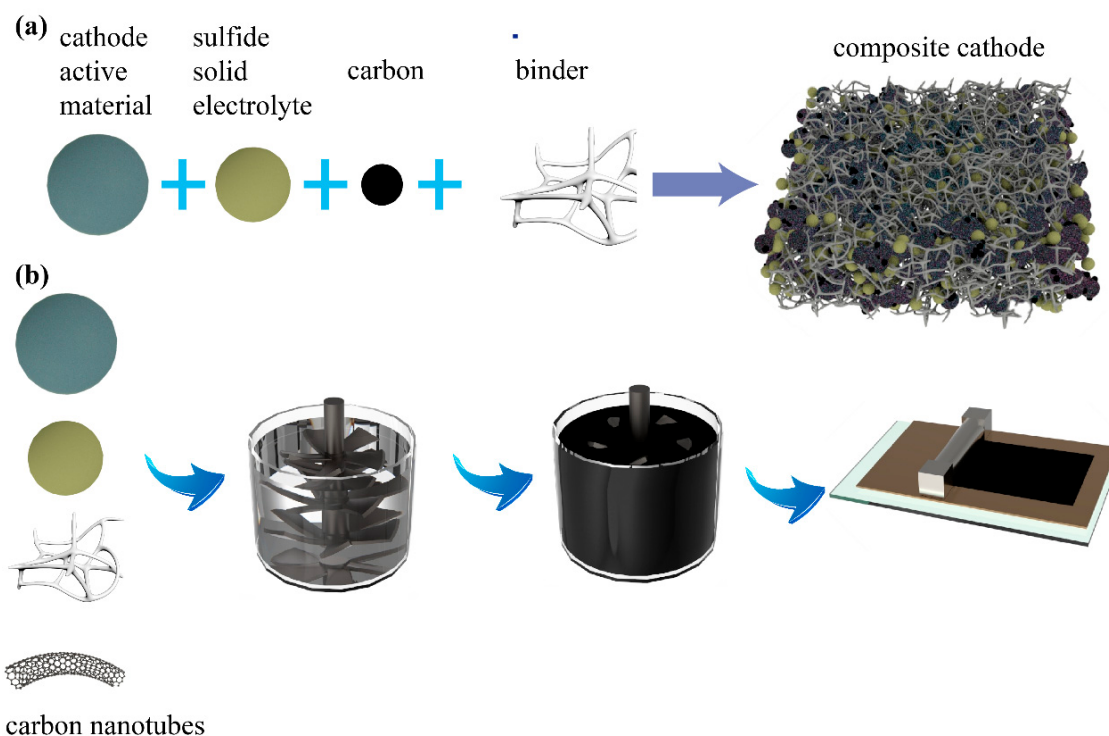


Figure 4. Schematic illustration of the preparation of composite cathode by (a) dry mixing and (b) tape-casting method.

5. Manufacturing of Anode

Recently, the anode materials used in solid-state batteries mainly include graphite, $\text{Li}_4\text{Ti}_5\text{O}_{12}$, silicon, lithium metal, and anode-free. The anode materials used in early SSBs are graphite and $\text{Li}_4\text{Ti}_5\text{O}_{12}$ [76]. The preparation method of composite anode is similar to that of the composite cathode, including the dry and wet processes. The dry process is that the graphite or $\text{Li}_4\text{Ti}_5\text{O}_{12}$, sulfide electrolyte and conductive carbon are mixed by ball milling to obtain the composite anode [15]. The wet method is that the binder is dissolved in a nonpolar or weakly polar solvent, and then the graphite or $\text{Li}_4\text{Ti}_5\text{O}_{12}$, sulfide electrolyte and conductive carbon are added into it, stirred, casted, and finally evaporated to obtain a composite anode [55]. Due to the low theoretical specific capacity of graphite (370 mAh g^{-1}) and $\text{Li}_4\text{Ti}_5\text{O}_{12}$ (175 mAh g^{-1}), the energy density of ASSBs is at most equal to that of liquid batteries, which does not reflect the advantages of ASSBs in terms of high specific energy.

To further improve the energy density of SSBs, lithium metal anode is considered as an ideal anode material due to its high theoretical specific capacity (3860 mAh g^{-1}), light weight, and low potential [28]. The electrochemical window of the sulfide solid electrolytes is narrow; therefore, when the sulfide electrolytes are in contact with lithium metal, they are easy to decompose, thereby increasing the interfacial resistance between the lithium anode and the sulfide solid electrolytes [27]. Due to the pores, cracks and high electronic conductivity of the sulfide solid electrolyte, the uneven plating and stripping of lithium ion will lead to lithium dendrites growth at large current densities, resulting in the short circuit of ASSBs [77–80]. Currently, Li-In alloy is widely used to replace lithium metal as anode, but the potential of Li-In alloy against lithium anode is 0.6 V , which will sacrifice the energy density of the whole cell [81]. In addition, the indium metal is relatively expensive; therefore, it is difficult for Li-In alloys to be commercially applied in ASSBs on a large scale.

To enable the utilization of lithium as anode in ASSBs, an ionically conducting and electronically insulating solid electrolyte interphase (SEI) layer formed in situ by doping the sulfide electrolyte with F^-/I^- , or preparing an artificial SEI layer on the surface of lithium anode, could improve the interfacial stability against lithium metal anode, and inhibit lithium dendrites growth to some extent [82–85]. When the areal capacity of the composite cathode is over 6 mAh cm^{-2} , the thickness of the required lithium anode is around $30 \mu\text{m}$. However, the lithium metal with a thickness of $100\text{--}500 \mu\text{m}$ is usually used in the laboratory, which is far from the practical application. Therefore, thick lithium metal needs to be rolled into thin lithium foils. Recently, China Energy Lithium Co., Ltd. (Tianjin, China) could produce continuous lithium foils with a thickness of $5\text{--}20 \mu\text{m}$. Due to the active nature of lithium chemistry, lithium production needs to be carried out in an inert atmosphere (such as Ar gas), and the assembly process of solid-state lithium metal battery also needs to be carried out in a dry room with a dew point of -40°C . Evaporating a layer of metal lithium on the surface of the composite electrolyte membrane can improve the interface contact between the lithium anode and the composite electrolyte membrane, and a lithium anode with controllable thickness will be realized, which will greatly improve the production efficiency of lithium anode compared with magnetron sputtering and pulsed laser deposition.

Anode-free batteries have received extensive attention, because they do not require additional lithium metal, which will greatly reduce the cost of lithium processing. Since only the current collector is used as the anode, the volumetric energy density of the whole cell will increase by 10%. Anode-free batteries will experience large-volume expansion during the first charge, and the Li^+ at the anode side is usually hard to completely return to the cathode side during the subsequent discharge process, leading to the formation of dead lithium, low Coulombic efficiency and capacity fading. Ag-C anode may help solve this problem. For example, Samsung assembled an ASSB with $\text{LiNi}_{0.90}\text{Co}_{0.05}\text{Mn}_{0.05}\text{O}_2$ cathode-active material, $\text{Li}_6\text{PS}_5\text{Cl}$ -based composite electrolyte membrane, and Ag-C anode. The hot isostatic pressing technique was also used to improve the physical contact between the electrodes and composite electrolyte membrane. The fabricated pouch cell exhibited

high energy density ($>900 \text{ Wh L}^{-1}$) and long cycle life (>1000 cycles) [86] (Figure 5a). Since Ag is relatively expensive, it is necessary to find cheaper metal elements to replace Ag.

Recently, compared with the lithium metal anode, silicon-based anode has also received extensive attention due to many advantages, such as comparable high specific capacity (3590 mAh g^{-1}), abundance of silicon element in the earth's crust, lower cost, higher stability against sulfide electrolytes, higher mechanical strength. ASSBs with silicon-based anode are expected to effectively avoid the lithium dendrites growth, and stable cycling at large current density and high areal capacity will be achieved [87]. Shirley et al. used PVDF binder to prepare a micron silicon anode sheet by wet method, and the composite anode did not contain conductive carbon and sulfide electrolyte. Carbon-free silicon electrodes will greatly reduce the decomposition of sulfide electrolytes, thereby improving the initial Coulombic efficiency and the rate performance of the cells. The ASSB could achieve a high areal capacity ($>1.5 \text{ mAh cm}^{-2}$) with a high capacity retention of 80% after 500 cycles (Figure 5b). Due to large volume expansion of pure silicon during cycling, the ASSBs need to be cycled under a large external pressure, which raises challenges for large-scale commercial applications [88]. Recently, Cao et al. mixed nano-silicon, sulfide electrolyte and carbon by ball milling to obtain the composite anode. The ASSB with $\text{LiNi}_{0.8}\text{Mn}_{0.1}\text{Co}_{0.1}\text{O}_2$ cathode and composite silicon anode shows a high capacity retention of 62% after 1000 cycles [89].

Considering the advantages and disadvantages of various anode materials, the application of lithium metal in ASSBs is an ideal target. However, there is no effective method to inhibit the lithium dendrites growth at large current densities. In the short term, silicon-based anodes are more likely to be used in ASSBs to achieve higher energy density and superior rate performance.

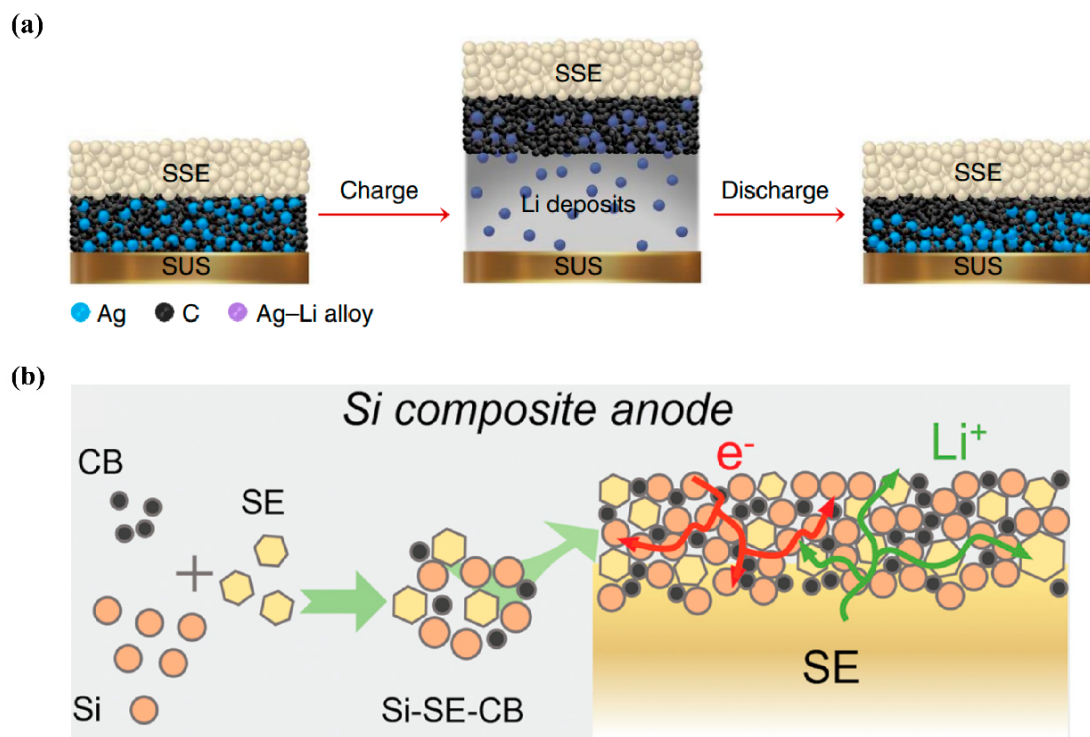


Figure 5. (a) Schematic illustration of lithium plating/stripping process of the Ag–C anode in an ASSB during cycling. Reproduced with permission from [86]. Copyright 2020, Springer Nature; (b) Schematic diagram of the preparation process of silicon–sulfide electrolyte–carbon black and the configuration of Si-based composite anode. Reproduced with permission from [89]. Copyright 2022, John Wiley and Sons.

6. Cell Assembly and Scaling up

One of the most popular ASSB assembly methods in the laboratory is lamination method, that is, the solid electrolyte layer is prepared by cold pressing, and then the composite cathode layer and composite anode layer are prepared on both sides of the solid electrolyte layer by cold pressing, respectively. For example, Kanno et al. dry-mixed LiCoO₂ coated with LiNbO₃, acetylene black with sulfide electrolyte (Li₁₀GeP₂S₁₂ or Li_{9.54}Si_{1.74}P_{1.44}S_{11.7}Cl_{0.3}) to obtain a composite cathode powder. Then the Li₄Ti₅O₁₂, solid electrolyte and acetylene black were mixed and ground in a mortar to obtain a composite anode powder. The solid electrolyte powder is pressed into pellets as the solid electrolyte layer, and then the composite cathode powder and composite anode powder are respectively pressed on both sides of the solid electrolyte layer to assemble an ASSB. The cell shows a good capacity retention of 75% after 500 cycles at a large current density of 18 C (charge/discharge time is 3 min) and at 100 °C [15]. The above battery assembly process is very complicated and difficult for continuous operation; therefore, it is not suitable for large-scale commercial mass production.

To maximize the utilization of production lines of commercial lithium-ion batteries, some researchers have proposed a method similar to liquid electrolyte injection in commercial lithium-ion batteries, that is, the sulfide electrolytes are dissolved into polar solvents, and then the solvent is injected into the electrode-separator assemblies in the conventional lithium-ion battery, and finally cured to obtain an ASSB. The cell delivers an initial discharge capacity of 109 mAh g⁻¹ at 70 °C [58]. With this method, the ionic conductivity of the sulfide electrolyte greatly decreases after being dissolved in a polar solvent, limiting the ionic transport of the cell. Therefore, a kind of sulfide electrolyte whose ionic conductivity could be recovered after dissolving in a polar solvent needs to be adopted.

To accelerate commercial applications, sulfide-based SSBs are developing from laboratory Swagelok cells to pouch cells. The specific preparation process of the pouch cell is as follows. First, the composite cathode slurry is cast on the aluminum current collector, and then the solid electrolyte slurry is cast on the composite cathode, and finally the lithium foil or the composite anode is stacked on the solid electrolyte layer to obtain an ASSB [90] (Figure 6a). When the solid electrolyte slurry is cast on the prepared composite cathode layer, interlayer mixing occurs easily between the solid electrolyte layer and preformed composite cathode layer [62]. Therefore, it is a good idea to prepare each layer separately like a liquid battery, and then they are stacked together to form an ASSBs. This method requires a freestanding solid electrolyte membrane. The composite cathode layer and the composite anode layer could also be prepared by dry process [49] (Figure 6b). To improve the physical contact between layers and reduce the porosity in each layer, uniaxial cold pressing or warm isostatic pressing can be carried out during cell assembly. Compared with uniaxial cold pressing, the effect of warm isostatic pressing is better; however, the operation process of warm isostatic pressing is complicated, leading to low efficiency and high cost, which is difficult to meet the requirements of mass production. When the cell size is larger, a larger tonnage equiaxed cold pressing machine is required to achieve densification [49]. Different from commercial lithium-ion batteries, bipolar stacking could be used in ASSBs, that is, both sides of the current collector could be coated with composite cathode slurry, which will further increase the specific energy and energy density of the cells [91]. However, the sulfide-based pouch cells are facing a serious problem that the electrode materials undergo large volume change during cycling, resulting in the mechanical contact loss at the electrode/electrolyte interface and rapid capacity decay. To ameliorate the large volume change of the electrode materials during cycling, the external fixture is usually used to apply stack pressure on the ASSBs, but the utilization of the bulky fixture will sacrifice the energy density of the whole cell [92]. Maintaining good contact at the electrode/electrolyte interface under lower external pressure is of great significance for improving the energy density and cycling performance of ASSBs.

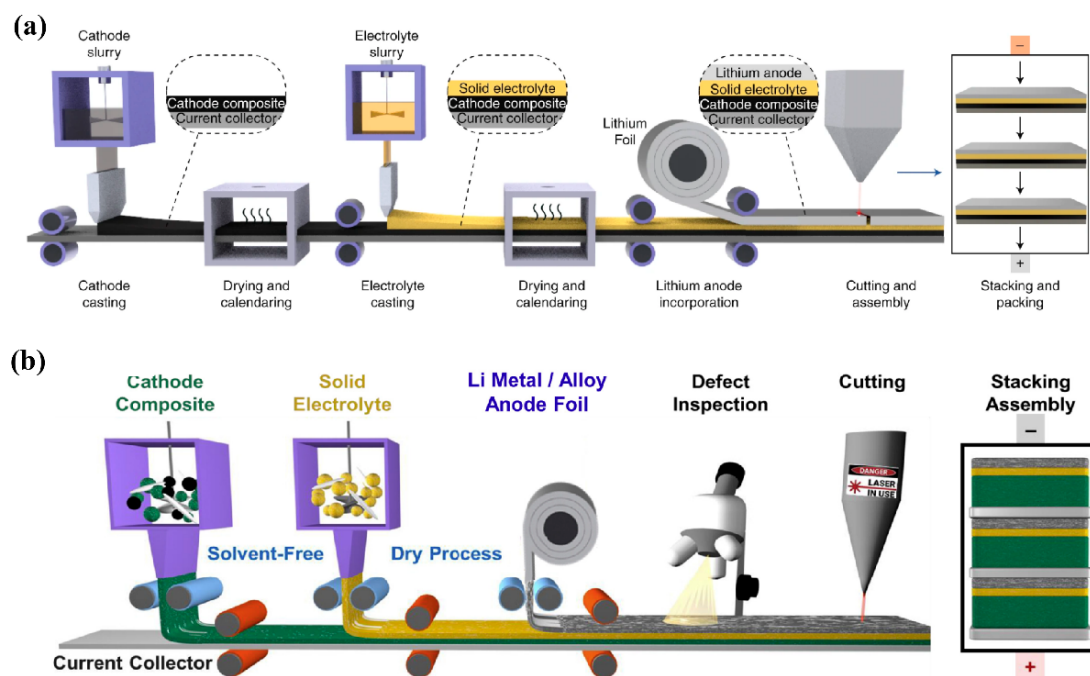


Figure 6. Schematic illustration of large-scale preparation of ASSBs. (a) the composite cathode slurry is tape-cast on the current collector, and then the composite electrolyte slurry is cast on the composite cathode, and finally the lithium foil is stacked to obtain an ASSB. Reproduced with permission from [90]. Copyright 2020, Springer Nature; (b) The composite cathode prepared by the solvent-free method is pressed onto the current collector, and then the composite electrolyte membrane is pressed onto the composite cathode, and finally the lithium foil/alloy anode is stacked to obtain an ASSB. Reproduced with permission from [49]. Copyright 2022, Elsevier B.V.

The most applicable method for large-scale assembly of ASSBs is as follows. First, the composite electrolyte layer and the composite electrode layers are prepared separately by tape-casting or dry process, and then these layers are stacked together and equiaxed cold-pressed, and finally the pouch cell is obtained.

7. Conclusions and Prospect

We systematically summarize the preparation methods of sulfide solid electrolyte powder, sulfide–polymer composite electrolyte membrane, composite cathode, composite anode and the assembly methods of ASSBs, analyze and compare the advantages and disadvantages of these methods in detail. Finally, we point out which kind of method shows good potential for large-scale application in ASSBs.

In terms of sulfide electrolytes, the recently prepared thiophosphate electrolytes show high ionic conductivity; however, the ionic conductivity will drop rapidly when they are exposed to moisture. Therefore, developing the sulfide solid electrolytes whose ionic conductivity remains above 6 mS cm^{-1} after exposed for 2 h in dry room (dew point -40°C) is of great significance for the practical application of ASSBs. We believe that solid-state reaction will be more applicable to large-scale manufacture sulfide electrolyte powders with high room-temperature ionic conductivity, but the particle size is relatively large. Wet milling could help reduce particle size but sacrifice ionic conductivity. In the future, if the particle size could be reduced via dry process to nanometer, dry process will be more competitive.

In terms of composite electrolyte membranes, preparing a composite electrolyte with a thickness less than $20 \mu\text{m}$ and an ionic conductivity higher than 4 mS cm^{-1} will help improve the specific energy of ASSBs. Tape-casting is a popular method that could be widely used to manufacture composite electrolyte membranes, but the room-temperature ionic conductivity is low due to the reaction with polar solvents. Optimizing the solvent-

binder pairing is an effective strategy. About the dry process, selecting polymers that could be fibrillated under shear force and stable against lithium anodes is essential. In the future, with the breakthrough of dry film preparation equipment and new binders, the dry process will replace the wet process as the mainstream technology for large-scale preparation of composite electrolyte membranes.

In terms of composite cathode, the traditional tape-casting method is a mainstream method. Due to ionically insulating binder and the side reactions between the sulfide electrolyte and the solvent, the effective ionic conductivity of the composite cathode is still low. In the future, it is necessary to find a better solvent-binder pairing, modify the existing binder to improve the adhesion between the electrodes and the current collector, which will help the composite cathode to achieve high effective ionic transport pathways. Meanwhile, with the breakthrough of dry cathode preparation equipment and new binder technology, dry-process electrode technology will be more competitive and widely used in ASSBs in the future.

In terms of anode, both lithium metal anode and silicon-based anode have shown promising prospects. The ultimate target is the utilization of lithium metal as anode. How to improve the interfacial stability between the sulfide electrolyte and the lithium anode needs to be investigated, which is of great significance for increasing the critical current density and inhibiting the lithium dendrite growth. However, there is a lack in effective methods to inhibit the lithium dendrites growth at large current densities. In the short term, silicon-based anodes are more likely to be used in ASSBs to achieve high specific energy and high power density. Regulating the ionic and electronic transport pathways of the silicon-sulfide electrolyte-conductive carbon composite anode, selecting a new binder to alleviate large volume change of silicon-based anode during charge and discharge process, or using Li-Si alloy will help improve the cycling life and capacity retention of ASSBs.

In terms of ASSB assembly, assembling pouch cells with composite electrodes and solid electrolyte layers stacked by equiaxed cold pressing is a promising technical route for large-scale manufacturing of sulfide-based ASSBs. The biggest challenge now is how to suppress the mechanical contact loss of the cell during cycling. The current mainstream method is to use a bulky device to apply high stack pressure on the ASSBs, which is obviously not suitable for large-scale manufacturing of ASSBs. In the future, developing new electrode materials with less strain, exploiting binders with soft and hard segments, constructing composite cathode with stronger structures, designing new external structure to lock the pressure inside the cell for suppressing the volume change of the electrode material during cycling, will help obtain an ASSB with long cycle life and high specific energy.

Author Contributions: Writing—original draft preparation, G.L. and Y.L.; writing—review and editing, S.W., Y.L. and Z.C.; supervision, project administration, S.W., J.F. and Z.C. All authors have read and agreed to the published version of the manuscript.

Funding: This work was funded by the Natural Science Foundation of Hubei Province (Grant No. 2022CFB760), Guangdong Basic and Applied Basic Research Foundation (Grant No. 2021A1515110312), Fundamental Research Funds for the Central Universities (WUT: 2022IVA005), the Key Scientific Research Project for Higher Education of Henan Province (22A530001), the Key Natural Science Foundation of Yibin Vocational & Technical College (21ZRZD-01), the Ph.D. Programs Foundation of Yibin Vocational & Technical College (ybzysc22bk01), Natural Science Foundation of Zhejiang Province (Grant No. LQ21E020006), the Fundamental Research Funds for the Provincial Universities of Zhejiang (Grant No. 2021YW46).

Data Availability Statement: Not applicable.

Conflicts of Interest: The authors declare no conflict of interest.

References

- Dunn, B.; Kamath, H.; Tarascon, J.-M. Electrical energy storage for the grid: A battery of choices. *Science* **2011**, *334*, 928–935. [[CrossRef](#)] [[PubMed](#)]
- Tran, M.; Banister, D.; Bishop, J.D.K.; McCulloch, M.D. Realizing the electric-vehicle revolution. *Nat. Clim. Change* **2012**, *2*, 328–333. [[CrossRef](#)]
- Choi, N.S.; Chen, Z.; Freunberger, S.A.; Ji, X.; Sun, Y.K.; Amine, K.; Yushin, G.; Nazar, L.F.; Cho, J.; Bruce, P.G. Challenges facing lithium batteries and electrical double-layer capacitors. *Angew. Chem. Int. Ed.* **2012**, *51*, 9994–10024. [[CrossRef](#)]
- Goodenough, J.B.; Kim, Y. Challenges for Rechargeable Li Batteries. *Chem. Mater.* **2009**, *22*, 587–603. [[CrossRef](#)]
- Xu, K. Electrolytes and interphases in Li-ion batteries and beyond. *Chem. Rev.* **2014**, *114*, 11503–11618. [[CrossRef](#)] [[PubMed](#)]
- Tarascon, J.-M.; Armand, M. Issues and challenges facing rechargeable lithium batteries. *Nature* **2001**, *414*, 359–367. [[CrossRef](#)]
- Choi, J.W.; Aurbach, D. Promise and reality of post-lithium-ion batteries with high energy densities. *Nat. Rev. Mater.* **2016**, *1*, 16013. [[CrossRef](#)]
- Chen, Y.; Wang, T.; Tian, H.; Su, D.; Zhang, Q.; Wang, G. Advances in lithium-sulfur batteries: From academic research to commercial viability. *Adv. Mater.* **2021**, *33*, e2003666. [[CrossRef](#)]
- Janek, J.; Zeier, W.G. Challenges in speeding up solid-state battery development. *Nat. Energy* **2023**, *8*, 230–240. [[CrossRef](#)]
- Zhou, L.; Minafra, N.; Zeier, W.G.; Nazar, L.F. Innovative approaches to Li-argyrodite solid electrolytes for all-solid-state lithium batteries. *Acc. Chem. Res.* **2021**, *54*, 2717–2728. [[CrossRef](#)]
- Ohno, S.; Banik, A.; Dewald, G.F.; Kraft, M.A.; Krauskopf, T.; Minafra, N.; Till, P.; Weiss, M.; Zeier, W.G. Materials design of ionic conductors for solid state batteries. *Prog. Energy* **2020**, *2*, 022001. [[CrossRef](#)]
- Jia, M.; Zhao, N.; Huo, H.; Guo, X. Comprehensive investigation into garnet electrolytes toward application-oriented solid lithium batteries. *Electrochem. Energy Rev.* **2020**, *3*, 656–689. [[CrossRef](#)]
- Huo, H.; Luo, J.; Thangadurai, V.; Guo, X.; Nan, C.-W.; Sun, X. Li_2CO_3 : A critical issue for developing solid garnet batteries. *ACS Energy Lett.* **2020**, *5*, 252–262. [[CrossRef](#)]
- Kamaya, N.; Homma, K.; Yamakawa, Y.; Hirayama, M.; Kanno, R.; Yonemura, M.; Kamiyama, T.; Kato, Y.; Hama, S.; Kawamoto, K.; et al. A lithium superionic conductor. *Nat. Mater.* **2011**, *10*, 682–686. [[CrossRef](#)] [[PubMed](#)]
- Kato, Y.; Hori, S.; Saito, T.; Suzuki, K.; Hirayama, M.; Mitsui, A.; Yonemura, M.; Iba, H.; Kanno, R. High-power all-solid-state batteries using sulfide superionic conductors. *Nat. Energy* **2016**, *1*, 16030. [[CrossRef](#)]
- Zhou, L.; Assoud, A.; Zhang, Q.; Wu, X.; Nazar, L.F. New family of argyrodite thioantimonate lithium superionic conductors. *J. Am. Chem. Soc.* **2019**, *141*, 19002–19013. [[CrossRef](#)] [[PubMed](#)]
- Lin, J.; Cherkashinin, G.; Schäfer, M.; Melinte, G.; Indris, S.; Kondrakov, A.; Janek, J.; Brezesinski, T.; Strauss, F. A high-entropy multicationic substituted lithium argyrodite superionic solid electrolyte. *ACS Mater. Lett.* **2022**, *4*, 2187–2194. [[CrossRef](#)]
- Lee, Y.; Jeong, J.; Lee, H.J.; Kim, M.; Han, D.; Kim, H.; Yuk, J.M.; Nam, K.-W.; Chung, K.Y.; Jung, H.-G.; et al. Lithium argyrodite sulfide electrolytes with high ionic conductivity and air stability for all-solid-state Li-ion batteries. *ACS Energy Lett.* **2021**, *7*, 171–179. [[CrossRef](#)]
- Masuda, N.; Kobayashi, K.; Utsuno, F.; Uchikoshi, T.; Kuwata, N. Effects of halogen and sulfur mixing on lithium-ion conductivity in $\text{Li}_{7-x-y}(\text{PS}_4)(\text{S}_{2-x-y}\text{Cl}_x\text{Br}_y)$ argyrodite and the mechanism for enhanced lithium conduction. *J. Phys. Chem. C* **2022**, *126*, 14067–14074. [[CrossRef](#)]
- Wu, J.; Liu, S.; Han, F.; Yao, X.; Wang, C. Lithium/Sulfide All-Solid-State Batteries using Sulfide Electrolytes. *Adv. Mater.* **2021**, *33*, 2000751. [[CrossRef](#)]
- Wang, Y.; Lv, Y.; Su, Y.; Chen, L.; Li, H.; Wu, F. 5V-class sulfurized spinel cathode stable in sulfide all-solid-state batteries. *Nano Energy* **2021**, *90*, 106589. [[CrossRef](#)]
- Wang, S.; Zhang, Y.; Zhang, X.; Liu, T.; Lin, Y.H.; Shen, Y.; Li, L.; Nan, C.W. High-conductivity argyrodite $\text{Li}_6\text{PS}_5\text{Cl}$ solid electrolytes prepared via optimized sintering processes for all-solid-state lithium-sulfur batteries. *ACS Appl. Mater. Interfaces* **2018**, *10*, 42279–42285. [[CrossRef](#)] [[PubMed](#)]
- Bielefeld, A.; Weber, D.A.; Janek, J. Modeling effective ionic conductivity and binder influence in composite cathodes for all-solid-state batteries. *ACS Appl. Mater. Interfaces* **2020**, *12*, 12821–12833. [[CrossRef](#)] [[PubMed](#)]
- Ohno, S.; Rosenbach, C.; Dewald, G.F.; Janek, J.; Zeier, W.G. Linking solid electrolyte degradation to charge carrier transport in the thiophosphate-based composite cathode toward solid-state lithium-sulfur batteries. *Adv. Funct. Mater.* **2021**, *31*, 2010620. [[CrossRef](#)]
- Minnmann, P.; Quillman, L.; Burkhardt, S.; Richter, F.H.; Janek, J. Editors' Choice—Quantifying the impact of charge transport bottlenecks in composite cathodes of all-solid-state batteries. *J. Electrochem. Soc.* **2021**, *168*, 040537. [[CrossRef](#)]
- Wang, S.; Xu, X.; Zhang, X.; Xin, C.; Xu, B.; Li, L.; Lin, Y.-H.; Shen, Y.; Li, B.; Nan, C.-W. High-performance $\text{Li}_6\text{PS}_5\text{Cl}$ -based all-solid-state lithium-ion batteries. *J. Mater. Chem. A* **2019**, *7*, 18612–18618. [[CrossRef](#)]
- Wang, S.; Fang, R.; Li, Y.; Liu, Y.; Xin, C.; Richter, F.H.; Nan, C.-W. Interfacial challenges for all-solid-state batteries based on sulfide solid electrolytes. *J. Mater.* **2021**, *7*, 209–218. [[CrossRef](#)]
- Hatzell, K.B.; Chen, X.C.; Cobb, C.L.; Dasgupta, N.P.; Dixit, M.B.; Marbella, L.E.; McDowell, M.T.; Mukherjee, P.P.; Verma, A.; Viswanathan, V.; et al. Challenges in lithium metal anodes for solid-state batteries. *ACS Energy Lett.* **2020**, *5*, 922–934. [[CrossRef](#)]
- Yang, M.; Chen, L.; Li, H.; Wu, F. Air/Water Stability Problems and Solutions for Lithium Batteries. *Energy Mater. Adv.* **2022**, *2022*, 9842651. [[CrossRef](#)]

30. Zhang, Z.; Kennedy, J.H. Synthesis and characterization of the B_2S_3 – Li_2S , the P_2S_5 – Li_2S and the B_2S_3 – P_2S_5 – Li_2S glass systems. *Solid State Ion.* **1990**, *38*, 217–224. [CrossRef]
31. Hirai, K.; Tatsumisago, M.; Minami, T. Thermal and electrical properties of rapidly quenched glasses in the systems Li_2S – SiS_2 – LixMOy ($\text{LixMOy} = \text{Li}_4\text{SiO}_4$, Li_2SO_4) *Solid State Ion.* **1995**, *78*, 269–273. [CrossRef]
32. Kanno, R.; Murayama, M. Lithium ionic conductor thio-LISICON: The Li_2S – GeS_2 – P_2S_5 system. *J. Electrochem. Soc.* **2001**, *148*, A742–A746. [CrossRef]
33. Minami, K.; Mizuno, F.; Hayashi, A.; Tatsumisago, M. Lithium ion conductivity of the Li_2S – P_2S_5 glass-based electrolytes prepared by the melt quenching method. *Solid State Ion.* **2007**, *178*, 837–841. [CrossRef]
34. Zhang, Y.; Chen, K.; Shen, Y.; Lin, Y.; Nan, C.-W. Synergistic effect of processing and composition x on conductivity of $x\text{Li}_2\text{S}$ –(100– x) P_2S_5 electrolytes. *Solid State Ion.* **2017**, *305*, 1–6. [CrossRef]
35. Miura, A.; Rosero-Navarro, N.C.; Sakuda, A.; Tadanaga, K.; Phuc, N.H.H.; Matsuda, A.; Machida, N.; Hayashi, A.; Tatsumisago, M. Liquid-phase syntheses of sulfide electrolytes for all-solid-state lithium battery. *Nat. Rev. Chem.* **2019**, *3*, 189–198. [CrossRef]
36. Indrawan, R.F.; Gamo, H.; Nagai, A.; Matsuda, A. Chemically understanding the liquid-phase synthesis of argyrodite solid electrolyte $\text{Li}_6\text{PS}_5\text{Cl}$ with the highest ionic conductivity for all-solid-state batteries. *Chem. Mater.* **2023**, *35*, 2549–2558. [CrossRef]
37. Rangasamy, E.; Liu, Z.; Gobet, M.; Pilar, K.; Sahu, G.; Zhou, W.; Wu, H.; Greenbaum, S.; Liang, C. An iodide-based $\text{Li}_7\text{P}_2\text{S}_8\text{I}$ superionic conductor. *J. Am. Chem. Soc.* **2015**, *137*, 1384–1387. [CrossRef] [PubMed]
38. Park, K.H.; Oh, D.Y.; Choi, Y.E.; Nam, Y.J.; Han, L.; Kim, J.Y.; Xin, H.; Lin, F.; Oh, S.M.; Jung, Y.S. Solution-processable glass LiI – Li_4SnS_4 superionic conductors for all-solid-state li-ion batteries. *Adv. Mater.* **2016**, *28*, 1874–1883. [CrossRef]
39. Mizuno, F.; Hayashi, A.; Tadanaga, K.; Tatsumisago, M. New, highly ion-conductive crystals precipitated from Li_2S – P_2S_5 glasses. *Adv. Mater.* **2005**, *17*, 918–921. [CrossRef]
40. Mizuno, F.; Hayashi, A.; Tadanaga, K.; Tatsumisago, M. High lithium ion conducting glass-ceramics in the system Li_2S – P_2S_5 . *Solid State Ion.* **2006**, *177*, 2721–2725. [CrossRef]
41. Jung, W.D.; Kim, J.S.; Choi, S.; Kim, S.; Jeon, M.; Jung, H.G.; Chung, K.Y.; Lee, J.H.; Kim, B.K.; Lee, J.H.; et al. Superionic halogen-rich Li-argyrodites using in situ nanocrystal nucleation and rapid crystal growth. *Nano Lett.* **2020**, *20*, 2303–2309. [CrossRef]
42. Yu, C.; van Eijck, L.; Ganapathy, S.; Wagemaker, M. Synthesis, structure and electrochemical performance of the argyrodite $\text{Li}_6\text{PS}_5\text{Cl}$ solid electrolyte for Li-ion solid state batteries. *Electrochim. Acta* **2016**, *215*, 93–99. [CrossRef]
43. Yu, C.; Li, Y.; Willans, M.; Zhao, Y.; Adair, K.R.; Zhao, F.; Li, W.; Deng, S.; Liang, J.; Banis, M.N.; et al. Superionic conductivity in lithium argyrodite solid-state electrolyte by controlled Cl-doping. *Nano Energy* **2020**, *69*, 104396. [CrossRef]
44. Kraft, M.A.; Ohno, S.; Zinkevich, T.; Koerver, R.; Culver, S.P.; Fuchs, T.; Senyshyn, A.; Indris, S.; Morgan, B.J.; Zeier, W.G. Inducing high ionic conductivity in the lithium superionic argyrodites $\text{Li}_{6+x}\text{P}_{1-x}\text{Ge}_x\text{S}_5\text{I}$ for all-solid-state batteries. *J. Am. Chem. Soc.* **2018**, *140*, 16330–16339. [CrossRef]
45. Wang, S.; Gautam, A.; Wu, X.; Li, S.; Zhang, X.; He, H.; Lin, Y.; Shen, Y.; Nan, C.-W. Effect of processing on structure and ionic conductivity of chlorine-rich lithium argyrodites. *Adv. Energy Sustain. Res.* **2023**, *2200197*. [CrossRef]
46. Minnmann, P.; Strauss, F.; Bielefeld, A.; Ruess, R.; Adelhelm, P.; Burkhardt, S.; Dreyer, S.L.; Trevisanello, E.; Ehrenberg, H.; Brezesinski, T.; et al. Designing cathodes and cathode active materials for solid-state batteries. *Adv. Energy Mater.* **2022**, *12*, 2201425. [CrossRef]
47. Wang, S.; Zhang, W.; Chen, X.; Das, D.; Ruess, R.; Gautam, A.; Walther, F.; Ohno, S.; Koerver, R.; Zhang, Q.; et al. Influence of crystallinity of lithium thiophosphate solid electrolytes on the performance of solid-state batteries. *Adv. Energy Mater.* **2021**, *11*, 2100654. [CrossRef]
48. Peng, L.; Yu, C.; Zhang, Z.; Xu, R.; Sun, M.; Zhang, L.; Cheng, S.; Xie, J. Tuning solid interfaces via varying electrolyte distributions enables high-performance solid-state batteries. *Energy Environ. Mater.* **2022**, *6*, e12308. [CrossRef]
49. Tan, D.H.S.; Meng, Y.S.; Jang, J. Scaling up high-energy-density sulfidic solid-state batteries: A lab-to-pilot perspective. *Joule* **2022**, *6*, 1755–1769. [CrossRef]
50. Villaluenga, I.; Wujcik, K.H.; Tong, W.; Devaux, D.; Wong, D.H.; DeSimone, J.M.; Balsara, N.P. Compliant glass–polymer hybrid single ion-conducting electrolytes for lithium batteries. *Proc. Natl. Acad. Sci. USA* **2016**, *113*, 52–57. [CrossRef]
51. Whiteley, J.M.; Taynton, P.; Zhang, W.; Lee, S.H. Ultra-thin solid-state li-ion electrolyte membrane facilitated by a self-healing polymer matrix. *Adv. Mater.* **2015**, *27*, 6922–6927. [CrossRef]
52. Zhang, Z.; Wu, L.; Zhou, D.; Weng, W.; Yao, X. Flexible sulfide electrolyte thin membrane with ultrahigh ionic conductivity for all-solid-state lithium batteries. *Nano Lett.* **2021**, *21*, 5233–5239. [CrossRef]
53. Wang, C.; Yu, R.; Duan, H.; Lu, Q.; Li, Q.; Adair, K.R.; Bao, D.; Liu, Y.; Yang, R.; Wang, J.; et al. Solvent-free approach for interweaving freestanding and ultrathin inorganic solid electrolyte membranes. *ACS Energy Lett.* **2021**, *7*, 410–416. [CrossRef]
54. Wang, S.; Zhang, X.; Liu, S.; Xin, C.; Xue, C.; Richter, F.; Li, L.; Fan, L.; Lin, Y.; Shen, Y.; et al. High-conductivity free-standing $\text{Li}_6\text{PS}_5\text{Cl}$ /poly(vinylidene difluoride) composite solid electrolyte membranes for lithium-ion batteries. *J. Mater.* **2020**, *6*, 70–76. [CrossRef]
55. Nam, Y.J.; Cho, S.J.; Oh, D.Y.; Lim, J.M.; Kim, S.Y.; Song, J.H.; Lee, Y.G.; Lee, S.Y.; Jung, Y.S. Bendable and thin sulfide solid electrolyte film: A new electrolyte opportunity for free-standing and stackable high-energy all-solid-state lithium-ion batteries. *Nano Lett.* **2015**, *15*, 3317–3323. [CrossRef]

56. Zhu, G.L.; Zhao, C.Z.; Peng, H.J.; Yuan, H.; Hu, J.K.; Nan, H.X.; Lu, Y.; Liu, X.Y.; Huang, J.Q.; He, C.; et al. A self-limited free-standing sulfide electrolyte thin film for all-solid-state lithium metal batteries. *Adv. Funct. Mater.* **2021**, *31*, 2101985. [[CrossRef](#)]
57. Cao, D.; Li, Q.; Sun, X.; Wang, Y.; Zhao, X.; Cakmak, E.; Liang, W.; Anderson, A.; Ozcan, S.; Zhu, H. Amphiphatic binder integrating ultrathin and highly ion-conductive sulfide membrane for cell-level high-energy-density all-solid-state batteries. *Adv. Mater.* **2021**, *33*, 2105505. [[CrossRef](#)]
58. Kim, D.H.; Lee, Y.-H.; Song, Y.B.; Kwak, H.; Lee, S.-Y.; Jung, Y.S. Thin and flexible solid electrolyte membranes with ultrahigh thermal stability derived from solution-processable Li argyrodites for all-solid-state Li-ion batteries. *ACS Energy Lett.* **2020**, *5*, 718–727. [[CrossRef](#)]
59. Liu, S.; Zhou, L.; Han, J.; Wen, K.; Guan, S.; Xue, C.; Zhang, Z.; Xu, B.; Lin, Y.; Shen, Y.; et al. Super long-cycling all-solid-state battery with thin $\text{Li}_6\text{PS}_5\text{Cl}$ -based electrolyte. *Adv. Energy Mater.* **2022**, *12*, 2200660. [[CrossRef](#)]
60. Shi, C.; Hamann, T.; Takeuchi, S.; Alexander, G.V.; Nolan, A.M.; Limpert, M.; Fu, Z.; O'Neill, J.; Godbey, G.; Dura, J.A.; et al. 3D asymmetric bilayer garnet-hybridized high-energy-density lithium-sulfur batteries. *ACS Appl. Mater. Interfaces* **2023**, *15*, 751–760. [[CrossRef](#)]
61. Shi, C.; Alexander, G.V.; O'Neill, J.; Duncan, K.; Godbey, G.; Wachsman, E.D. All-solid-state garnet type sulfurized polyacrylonitrile/lithium-metal battery enabled by an inorganic lithium conductive salt and a bilayer electrolyte architecture. *ACS Energy Lett.* **2023**, *8*, 1803–1810. [[CrossRef](#)]
62. Lee, J.; Lee, T.; Char, K.; Kim, K.J.; Choi, J.W. Issues and advances in scaling up sulfide-based all-solid-state batteries. *Acc. Chem. Res.* **2021**, *54*, 3390–3402. [[CrossRef](#)] [[PubMed](#)]
63. Tan, D.H.S.; Banerjee, A.; Deng, Z.; Wu, E.A.; Nguyen, H.; Doux, J.-M.; Wang, X.; Cheng, J.-H.; Ong, S.P.; Meng, Y.S.; et al. Enabling thin and flexible solid-state composite electrolytes by the scalable solution process. *ACS Appl. Energy Mater.* **2019**, *2*, 6542–6550. [[CrossRef](#)]
64. Kim, S.; Chart, Y.A.; Narayanan, S.; Pasta, M. Thin solid electrolyte separators for solid-state lithium-sulfur batteries. *Nano Lett.* **2022**, *22*, 10176–10183. [[CrossRef](#)]
65. Zhao, X.; Xiang, P.; Wu, J.; Liu, Z.; Shen, L.; Liu, G.; Tian, Z.; Chen, L.; Yao, X. Toluene tolerated $\text{Li}_{9.88}\text{GeP}_{1.96}\text{Sb}_{0.04}\text{S}_{11.88}\text{Cl}_{0.12}$ solid electrolyte toward ultrathin membranes for all-solid-state lithium batteries. *Nano Lett.* **2023**, *23*, 227–234. [[CrossRef](#)]
66. Liu, X.; Zheng, B.; Zhao, J.; Zhao, W.; Liang, Z.; Su, Y.; Xie, C.; Zhou, K.; Xiang, Y.; Zhu, J.; et al. Electrochemo-mechanical effects on structural integrity of Ni-rich cathodes with different microstructures in all solid-state batteries. *Adv. Energy Mater.* **2021**, *11*, 2003583. [[CrossRef](#)]
67. Santhosha, A.L.; Nazer, N.; Koerver, R.; Randau, S.; Richter, F.H.; Weber, D.A.; Kulisch, J.; Adermann, T.; Janek, J.; Adelhelm, P. Macroscopic displacement reaction of copper sulfide in lithium solid-state batteries. *Adv. Energy Mater.* **2020**, *10*, 2002394. [[CrossRef](#)]
68. Han, F.; Yue, J.; Fan, X.; Gao, T.; Luo, C.; Ma, Z.; Suo, L.; Wang, C. High-performance all-solid-state lithium-sulfur battery enabled by a mixed-conductive Li_2S nanocomposite. *Nano Lett.* **2016**, *16*, 4521–4527. [[CrossRef](#)]
69. Zhang, Q.; Cao, D.; Ma, Y.; Natan, A.; Aurora, P.; Zhu, H. Sulfide-based solid-state electrolytes: Synthesis, stability, and potential for all-solid-state batteries. *Adv. Mater.* **2019**, *31*, 1901131. [[CrossRef](#)]
70. Cao, D.; Zhang, Y.; Nolan, A.M.; Sun, X.; Liu, C.; Sheng, J.; Mo, Y.; Wang, Y.; Zhu, H. Stable thiophosphate-based all-solid-state lithium batteries through conformally interfacial nanocoating. *Nano Lett.* **2020**, *20*, 1483–1490. [[CrossRef](#)]
71. Ohno, S.; Koerver, R.; Dewald, G.; Rosenbach, C.; Titscher, P.; Steckermeier, D.; Kwade, A.; Janek, J.; Zeier, W.G. Observation of chemomechanical failure and the influence of cutoff potentials in all-solid-state Li-S batteries. *Chem. Mater.* **2019**, *31*, 2930–2940. [[CrossRef](#)]
72. Wang, S.; Tang, M.; Zhang, Q.; Li, B.; Ohno, S.; Walther, F.; Pan, R.; Xu, X.; Xin, C.; Zhang, W.; et al. Lithium argyrodite as solid electrolyte and cathode precursor for solid-state batteries with long cycle life. *Adv. Energy Mater.* **2021**, *11*, 2101370. [[CrossRef](#)]
73. Hippauf, F.; Schumm, B.; Doerfler, S.; Althues, H.; Fujiki, S.; Shiratsuchi, T.; Tsujimura, T.; Aihara, Y.; Kaskel, S. Overcoming binder limitations of sheet-type solid-state cathodes using a solvent-free dry-film approach. *Energy Storage Mater.* **2019**, *21*, 390–398. [[CrossRef](#)]
74. Kim, D.H.; Lee, H.A.; Song, Y.B.; Park, J.W.; Lee, S.-M.; Jung, Y.S. Sheet-type $\text{Li}_6\text{PS}_5\text{Cl}$ -infiltrated Si anodes fabricated by solution process for all-solid-state lithium-ion batteries. *J. Power Sources* **2019**, *426*, 143–150. [[CrossRef](#)]
75. Oh, D.Y.; Kim, D.H.; Jung, S.H.; Han, J.-G.; Choi, N.-S.; Jung, Y.S. Single-step wet-chemical fabrication of sheet-type electrodes from solid-electrolyte precursors for all-solid-state lithium-ion batteries. *J. Mater. Chem. A* **2017**, *5*, 20771–20779. [[CrossRef](#)]
76. Nam, Y.J.; Oh, D.Y.; Jung, S.H.; Jung, Y.S. Toward practical all-solid-state lithium-ion batteries with high energy density and safety: Comparative study for electrodes fabricated by dry- and slurry-mixing processes. *J. Power Sources* **2018**, *375*, 93–101. [[CrossRef](#)]
77. Porz, L.; Swamy, T.; Sheldon, B.W.; Rettenwander, D.; Frömling, T.; Thaman, H.L.; Berendts, S.; Uecker, R.; Carter, W.C.; Chiang, Y.M. Mechanism of lithium metal penetration through inorganic solid electrolytes. *Adv. Energy Mater.* **2017**, *7*, 1701003. [[CrossRef](#)]
78. Kasemchainan, J.; Zekoll, S.; Jolly, D.S.; Ning, Z.; Hartley, G.O.; Marrow, J.; Bruce, P.G. Critical stripping current leads to dendrite formation on plating in lithium anode solid electrolyte cells. *Nat. Mater.* **2019**, *18*, 1105–1111. [[CrossRef](#)]
79. Ning, Z.; Jolly, D.S.; Li, G.; De Meyere, R.; Pu, S.D.; Chen, Y.; Kasemchainan, J.; Ihli, J.; Gong, C.; Liu, B.; et al. Visualizing plating-induced cracking in lithium-anode solid-electrolyte cells. *Nat. Mater.* **2021**, *20*, 1121–1129. [[CrossRef](#)]
80. Han, F.; Westover, A.S.; Yue, J.; Fan, X.; Wang, F.; Chi, M.; Leonard, D.N.; Dudney, N.J.; Wang, H.; Wang, C. High electronic conductivity as the origin of lithium dendrite formation within solid electrolytes. *Nat. Energy* **2019**, *4*, 187–196. [[CrossRef](#)]

81. Santhosha, A.L.; Medenbach, L.; Buchheim, J.R.; Adelhelm, P. The indium–lithium electrode in solid-state lithium-ion batteries: Phase formation, redox potentials, and interface stability. *Batter. Supercaps* **2019**, *2*, 524–529. [[CrossRef](#)]
82. Huo, H.; Jiang, M.; Mogwitz, B.; Sann, J.; Yusim, Y.; Zuo, T.T.; Moryson, Y.; Minnmann, P.; Richter, F.H.; Veer Singh, C.; et al. Interface Design Enabling Stable Polymer/Thiophosphate Electrolyte Separators for Dendrite-Free Lithium Metal Batteries. *Angew Chem. Int. Ed.* **2023**, *62*, e202218044. [[CrossRef](#)]
83. Xu, R.; Han, F.; Ji, X.; Fan, X.; Tu, J.; Wang, C. Interface engineering of sulfide electrolytes for all-solid-state lithium batteries. *Nano Energy* **2018**, *53*, 958–966. [[CrossRef](#)]
84. Fan, X.; Ji, X.; Han, F.; Yue, J.; Chen, J.; Chen, L.; Deng, T.; Jiang, J.; Wang, C. Fluorinated solid electrolyte interphase enables highlyreversible solid-state Li metal battery. *Sci. Adv.* **2018**, *4*, eaau9245. [[CrossRef](#)]
85. Liang, J.; Li, X.; Zhao, Y.; Goncharova, L.V.; Li, W.; Adair, K.R.; Banis, M.N.; Hu, Y.; Sham, T.K.; Huang, H.; et al. An air-stable and dendrite-free li anode for highly stable all-solid-state sulfide-based li batteries. *Adv. Energy Mater.* **2019**, *9*, 1902125. [[CrossRef](#)]
86. Lee, Y.-G.; Fujiki, S.; Jung, C.; Suzuki, N.; Yashiro, N.; Omoda, R.; Ko, D.-S.; Shiratsuchi, T.; Sugimoto, T.; Ryu, S.; et al. High-energy long-cycling all-solid-state lithium metal batteries enabled by silver–carbon composite anodes. *Nat. Energy* **2020**, *5*, 299–308. [[CrossRef](#)]
87. Huo, H.; Janek, J. Silicon as emerging anode in solid-state batteries. *ACS Energy Lett.* **2022**, *7*, 4005–4016. [[CrossRef](#)]
88. Tan, D.H.S.; Chen, Y.-T.; Yang, H.; Bao, W.; Sreenarayanan, B.; Doux, J.-M.; Li, W.; Lu, B.; Ham, S.-Y.; Sayahpour, B.; et al. Carbon-free high-loading silicon anodes enabled by sulfide solid electrolytes. *Science* **2021**, *373*, 1494–1499. [[CrossRef](#)] [[PubMed](#)]
89. Cao, D.; Sun, X.; Li, Y.; Anderson, A.; Lu, W.; Zhu, H. Long-cycling sulfide-based all-solid-state batteries enabled by electrochemomechanically stable electrodes. *Adv. Mater.* **2022**, *34*, 2200401. [[CrossRef](#)]
90. Tan, D.H.S.; Banerjee, A.; Chen, Z.; Meng, Y.S. From nanoscale interface characterization to sustainable energy storage using all-solid-state batteries. *Nat. Nanotechnol.* **2020**, *15*, 170–180. [[CrossRef](#)] [[PubMed](#)]
91. Cao, D.; Sun, X.; Wang, Y.; Zhu, H. Bipolar stackings high voltage and high cell level energy density sulfide based all-solid-state batteries. *Energy Storage Mater.* **2022**, *48*, 458–465. [[CrossRef](#)]
92. Doux, J.M.; Nguyen, H.; Tan, D.H.S.; Banerjee, A.; Wang, X.; Wu, E.A.; Jo, C.; Yang, H.; Meng, Y.S. Stack pressure considerations for room-temperature all-solid-state lithium metal batteries. *Adv. Energy Mater.* **2019**, *10*, 1903253. [[CrossRef](#)]

Disclaimer/Publisher’s Note: The statements, opinions and data contained in all publications are solely those of the individual author(s) and contributor(s) and not of MDPI and/or the editor(s). MDPI and/or the editor(s) disclaim responsibility for any injury to people or property resulting from any ideas, methods, instructions or products referred to in the content.